Free-Space and Intermolecular Interaction Effects on the Local-Chain Rotational Relaxation Dynamics in Dye + Polymer Lasing Materials

ARTICLE *in* MACROMOLECULES · FEBRUARY 2004

Impact Factor: 5.8 · DOI: 10.1021/ma035299v

3 AUTHORS:

Ioannis M. Kalogeras
National and Kapodistrian University of Athens
40 PUBLICATIONS **587** CITATIONS
SEE PROFILE

E.R. Neagu
New University of Lisbon
137 PUBLICATIONS **1,329** CITATIONS
SEE PROFILE

Aglaia Vassilikou-Dova
National and Kapodistrian University of Athens
69 PUBLICATIONS **495** CITATIONS
SEE PROFILE

Free-Space and Intermolecular Interaction Effects on the Local-Chain Rotational Relaxation Dynamics in Dye + Polymer Lasing Materials

Ioannis M. Kalogeras,*,† Eugen R. Neagu,‡ and Aglaia Vassilikou-Dova†

Department of Physics, Section of Solid State Physics, University of Athens, Panepistimiopolis, 157 84 Zografos, Hellas, Greece, and Department of Physics, Technical University of Iasi, B-dul D. Mangeron N. 67, OP 10, CP 2000, Iasi-6600, Romania

Received September 3, 2003; Revised Manuscript Received September 21, 2003

ABSTRACT: Dielectric relaxation spectroscopy (DRS) and thermally stimulated depolarization currents (TSDC) are combined to analyze the secondary (β) side-chain relaxation mode of poly(methyl methacrylate) (PMMA) in conventional solid-state laser matrices. The response of undoped PMMA is compared with that of mixtures with fluorescent dyes: the highly polar and ionic rhodamine 6G/Cl^- and pyrromethene 567 dyes and the neutral and apolar substituted perylene and perylimides. Variations in characteristic features of the β relaxation, such as the spectral position and the relative strength of the thermocurrent and dielectric loss bands as well as the absolute values and the width of the distribution in apparent activation energies (E_a), are exploited to isolate different types of intermolecular and intramolecular guest−host interactions. The results are interpreted in view of opposing effects on the relaxation characteristics of the pendant groups. In the presence of the perylene/perylimide dyes the β process is mainly influenced by variations in the local free space: by increasing the size of the dye molecule, the (re)orientation of the ester carbonyl side groups is more effectively hindered (i.e., increased E_a and antiplasticization). In contrast, in the xanthene/pyrromethene + PMMA mixtures, dipole−dipole and electrostatic interactions and charge-transfer reactions may be considered to control the dynamics of the β relaxation mode. The complementary character of the two dielectric techniques and possible relationships between the dielectric results and optical characteristics of each blend are discussed.

1. Introduction

From the mid-1960s[1] dye lasers have been attractive sources of coherent radiation with unique operational flexibility[2] and wavelength coverage from the ultraviolet to infrared. Organic compounds have been demonstrated to lase in the gas,[3] the liquid, and the solid states.[1,4] Nevertheless, it is in the liquid phase that dyes have been most frequently used in laser devices. This is mainly due to the outstanding performance of such systems, operating from continuous-wave to mode-locked picosecond regimes and from low to high average powers with minimized heat dissipation problems and the significantly reduced cost for the laser system. Still, in liquid solutions a number of thermodynamic, spectroscopic, and kinetic properties of the dye may be adversely influenced. For example, both lasing efficiency and photostability show strong dependence on the solvent polarity and to a lower extent its hydrogen- or electron-donating properties.[2] In addition, practical disadvantages of the liquid systems, such as the toxicity and flammability of several dyes and the need for large volumes of organic solvents, have moved scientific interest toward the implementation of solid-state dye laser (SSDL) systems.[5]

Irrespective of the industrial application involved, the determining factor for the successful implementation of an optical system is the selection of the appropriate combination of the dye molecule (guest) and the host matrix. They had to pass nearly two decades since the late 1960s, where Soffer and Mcfarland[6] and Peterson and Snavely[7] demonstrated stimulated emission from polymeric matrices encapsulating organic dyes, before significant breakthroughs in the development of modified polymers with improved laser-radiation-damage thresholds resulted to practical SSDLs. Over the past decades, several organic substances with optical functions, such as fluorescence, phosphorescence, photoconductivity, laser oscillation, and nonlinear optical properties, have been incorporated into various solid-state hosts, i.e., electrooptical inorganic compounds (e.g., KH_2PO_4, $LiNbO_3$, and GaAs), sol−gel process derived inorganic glasses (SiO_2 gels, silica−zirconia, Al_2O_3 gels, etc.),[8,9] and polycom glasses and organically modified silicates.[10] Transparent polymers have been extensively used as dye-caging materials. Some representative examples are the epoxy resins,[11] poly(vinylpyridine),[12] poly(vinyl alcohol),[13] polyethylene,[14] poly(methacrylic acid),[15] poly(vinyl acetate),[16] poly(methyl methacrylate) (PMMA),[17−21] and matrices of methyl methacrylate (MMA) with different comonomers.[22−24] Measuring optical characteristics, like optical scattering, fluorescence quantum yield, efficiency, tunability in pump wavelength, and photostability, has rigorously tested the above matrices.

The polyacrylic polymer PMMA is the basis for the development of various complex systems with immobilized photochromic and lasing molecules. Typical commercial applications of such systems cover diverse areas: atmospheric and underwater sensing, local area communication networks, medicine, isotope separation, and spectroscopy. Recent applications extend to fiber-optic humidity sensors,[25] optical memory materials for computer data storage,[26,27] neutron radiation dosimeters,[26] advanced luminescent solar concentrators,[28,29] and photonic crystals (e.g., dye + PMMA opaline films consisting of well-ordered packages of beads that can be precisely patterned by e-beam lithography[30]).

The excellent optical transparency of PMMA makes it an obligatory reference in any strategy directed to

† University of Athens.
‡ Technical University of Iasi.
* Corresponding author: e-mail ikaloger@cc.uoa.gr.

10.1021/ma035299v CCC: $27.50
Published on Web 01/06/2004

improve lasing performance in polymeric SSDLs. For example, appropriate modifications of PMMA have been found to improve lasing efficiency while maintaining photostability.[31] Both parameters seem to improve by optimizing the free space by controlled cross-linking of the polymer chains.[32] It appears that further improvements would require a greater understanding of the interactions and the degradation mechanisms involved when the fluorophores are embedded in the solid matrices and their dependence on the polymeric composition. Analysis of the dielectric signature of the molecular relaxation mechanisms in dye + polymer blends is expected to shed light on physical and chemical factors determining their optical characteristics. Hitherto, there is a limited number of dielectric reports performed on radical polymerization or solvent casting prepared PMMA containing rhodamine B,[33] rhodamine 6G,[33−35] K1,[33] coumarin 6,[36,37] substituted perylenes,[34,35,38,39] fluorescein−Na,[36,37] and the azo-dye DR-1.[40] In these studies, attempts were made to relate the changes in the relaxation parameters of the primary (α) or the secondary (β) dielectric relaxation modes of PMMA (e.g., the activation energy E_a, the distribution of the relaxation times τ, and the dielectric strength $\Delta\epsilon$) with intermolecular guest−host interactions. Analogous information has been provided by studies on the influence of the matrix to the orientational dynamics of the chromophores in nonlinear optical polymers.[41−43]

In this article we present a dielectric study of the β relaxation mechanism in dye + PMMA solid solutions. In relation to earlier reports,[33−40] the present study presents several advantages. For the first time a wide range of dispersed laser-active organic dyes with varied polarity, ionicity, and size are simultaneously studied (Figure 1): a brominated perylene (perylene green, PG), two perylimides (perylimide orange, PO; perylimide red, PR), a typical pyrromethene−BF_2 type dye (pyrromethene 567, PM-567), and a benchmark xanthene dye (rhodamine 6G chloride, Rh 6G/Cl^-). Dielectric data for the mixtures of PMMA with PR and PM-567 will be reported for the first time. Moreover, results obtained by means of two well-established complementary dielectric methods, thermally stimulated depolarization currents (TSDC) and dielectric relaxation spectroscopy (DRS), are compared. This combination permits the quantitative study of counteracting effects of blending on the relaxation characteristics (τ, E_a, $\Delta\epsilon$) of the β process. The importance of the various types of physical and chemical guest−host interactions and some aspects of their lasing action will be cross-examined.

2. Experimental Section

2.1. Materials. Commercially supplied MMA was washed three times in 5% NaOH and 20% NaCl in water to free it from its inhibitor, hydroquinone monomethyl ether, followed by repeated washing with distilled water, and then dried with anhydrous sodium sulfate. Prior to polymerization, the chemically pure liquid monomer was stored at $T < 273$ K to minimize spontaneous polymerization effects. Free radical polymerization was performed at 413 K for 3 days, initiated by 0.1% by mass of benzoyl peroxide dissolved into MMA. High-resolution proton nuclear magnetic resonance (NMR) measurements indicate a random stereochemistry of the tertiary carbons in the macromolecules with ~50% syndio-triad content. An X-ray diffraction (XRD) study verified the absence of the crystalline phase.

The incorporation of the dyes in PMMA was performed following two different procedures. The apolar and neutral substituted perylenes (PG, PO, and PR;[44] Figure 1) were dissolved into the liquid monomer−initiator mixture, and the mixture was polymerized as above. The estimated dye concentrations (C) in the dye solutions are $C_{PG} = 10^{-4}$ mol/L, $C_{PO} = 8 \times 10^{-5}$ mol/L, and $C_{PR} = 10^{-4}$ mol/L. The highly ionic and polar xanthene dye rhodamine 6G chloride (Rh 6G) is only slightly soluble in the less polar MMA solution. Thus, Rh 6G + PMMA was prepared by adding solution of the dye in ethyl alcohol (EtOH) in the initiator/monomer mixture (8% of 10^{-3} mol/L dye solution in ethanol and 92% MMA), and radical polymerization was performed as above. The estimated dye concentration is $C_{Rh6G} = 8 \times 10^{-5}$ mol/L. A similar procedure was used to incorporate PM-567 in PMMA. Because of dye degradation (detected by the partial decoloration of the solid solution relative to the initial liquid mixture), the concentration of PM-567 in the polymer matrix has not been determined ($C_{PM} < 8 \times 10^{-5}$ mol/L).

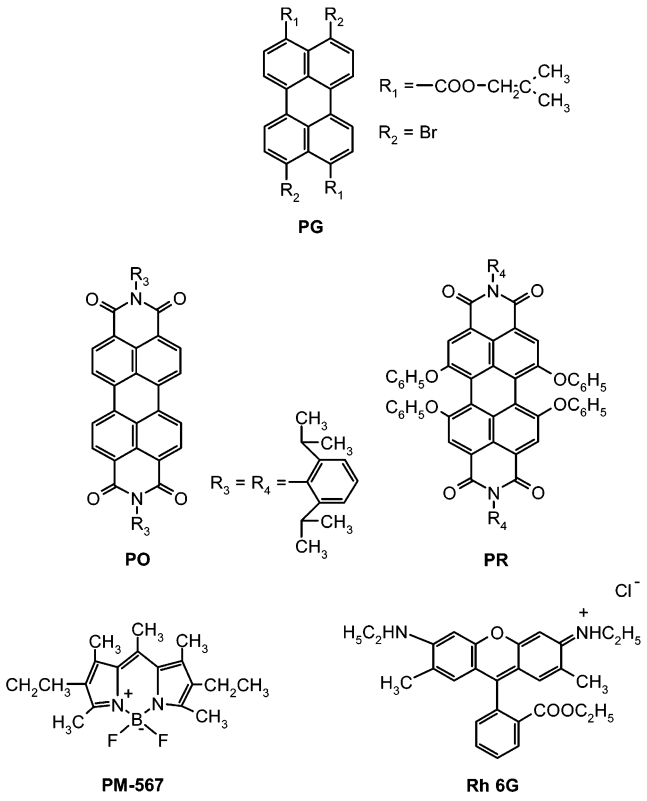

Figure 1. Molecular structure of the dyes: perylene green (PG), perylimide orange (PO, KF 241), perylimide red (PR, KF 856), pyrromethene 567 (PM-567), and rhodamine 6G/Cl^- (Rh 6G).

To minimize the influence of the solvent on the dielectric response of the polymeric matrix, the samples, prior to the experiments, underwent vacuum and/or heat treatments (at 320 K). However, appreciable traces of EtOH and adsorbed water are expected to reside in relatively strong "binding sites", e.g., hydrogen bonded to C=O groups. The number of these ester carbonyls is considered insignificant when compared to the overall amount of the polar side chains in PMMA. Accordingly, we expect them to have a negligible effect on the response recorded for the β relaxation signal.

2.2. Methods. Dielectric relaxation may be defined as approach to equilibrium of a system driven out of equilibrium by a time-dependent perturbation, i.e., an electric field $E(t)$. For an arbitrary history of the perturbation, a change in a related variable describing the state of the system, i.e., of the polarization P, is observed. By applying Boltzmann's superposition principle, $E(t)$ and $P(t)$ are related by the expression

$$E(t) = \int_0^t \frac{dP(u)}{du} \psi(t-u)\, du \qquad (1)$$

For amorphous substances the overall system response is non-Debye; i.e., the time-domain relaxation function $\psi(t)$ departs from the form

$$\psi(t) = \psi(0)\exp\left(-\frac{t}{\tau}\right) \tag{2}$$

since individual processes have different relaxation times τ.

In the time scale greater than ~100 μs (covered by DRS) two processes can be observed: the translational motion of charges through the electrode/sample/electrode system that result in a direct current density $j = \sigma E$ (σ being the conductivity) and short-range motions of charges (i.e., (re)-orientational motions of ions, molecules, or of defects with inherent electric dipole moment) that lead to a displacement current density given by $j = \mathrm{d}D/\mathrm{d}t$ (D being the dielectric displacement). In general, the dielectric polarization processes are frequency-dependent and show relaxation phenomena with varying frequency. The relaxation processes are described by the complex dielectric permittivity $\epsilon^*(\omega)$

$$\epsilon^*(\omega) = \epsilon'(\omega) - i\epsilon''(\omega) \tag{3}$$

where $\epsilon'(\omega)$ is the real part of the dielectric permittivity, $\epsilon''(\omega)$ is the dielectric loss, $\omega = 2\pi f$ is the angular frequency, f is the frequency, and i is the imaginary unit ($= \sqrt{-1}$). The experimental data are usually fitted by the assumption that the total dielectric response is the linear superposition of the contribution from the dc conductivity (σ_0) and different polarization processes expressed by their complex dielectric constant $\Delta\epsilon_i^*(\omega)$ in the form of the phenomenological asymmetric Havriliak−Negami function (HN function)

$$\epsilon^*_{\mathrm{exp}} = \frac{\sigma_0}{\omega\epsilon_0} + \epsilon_\infty + \sum_i \frac{\Delta\epsilon_i}{[1 - (i\omega\tau_i)^{\alpha_{\mathrm{HN},i}}]^{\beta_{\mathrm{HN},i}}} \tag{4}$$

where ϵ_0 is the permittivity of the vacuum and ϵ_∞ the limiting value at high frequencies of the real part of the permittivity. In the framework of the HN function, the temperature-dependent parameters of each individual relaxation process are the relaxation time $\tau(T)$, the relaxation strength $\Delta\epsilon(T)$, the width ($1 - \alpha_{\mathrm{HN}}$), and the asymmetry β_{HN} of the relaxation in relation to a Debye-like process with $\alpha = \beta = 1$. The relaxation times τ_i determine the positions of each process in the time or the frequency scale due to the connection of each relaxation time with the frequency of the maximum of the corresponding loss peak: $\omega_{\mathrm{m},i} = 1/\tau_i$. For relaxations activating below the glass-transition temperature of a polymer the thermally activated relaxation time can be expressed by the Arrhenius equation

$$\tau(T) = \tau_0\exp\left(\frac{E_\mathrm{a}}{k_\beta T}\right) \tag{5}$$

where τ_0 is related to the inverse of the characteristic vibration frequency at infinite temperature of a charge carrier trapped in its site, and k_β is Boltzmann's constant. The relaxation parameters (E_a, τ_0) can be deduced from the slope and intercept, respectively, of the linear plot of $\ln(\omega_\mathrm{m})$ vs $1/T$ (Arrhenius plots) or by fitting the experimental data to eq 5.

As an alternative to DRS, the thermally stimulated depolarization currents technique[44−46] is used to separate and study dielectrically active relaxation phenomena. The technique is widely recognized as an efficient route for the determination of intra- and intermolecular interactions in polymers. The TSDC experiment consists of the polarization of the sample at some sufficiently high temperature T_p by applying a static electric field E_p for a sufficient period of time t_p. When the temperature of the sample is lowered to T_0 with the electric field applied and then shortened at T_0, the nonequilibrium state of the system is frozen in. During the successive heating, the recovery of the system is monitored by measuring the depolarization current density

$$j(T) = \frac{P_0(T_P)}{\tau(T)}\exp\left[-\frac{1}{b}\int_{T_0}^{T}\frac{\mathrm{d}T'}{\tau(T')}\right] \tag{6}$$

where P_0 is the saturation polarization and $b = \mathrm{d}T/\mathrm{d}t$ the constant heating rate. The following equation is used to calculate $\tau(T)$ from TSDC experimental data:

$$\tau(T) = \frac{P(T)}{j(T)} = \frac{\frac{1}{b}\int_{T_0}^{T_\infty} j(T')\,\mathrm{d}T'}{j(T)} \tag{7}$$

The parameters (E_a, τ_0) can be obtained by fitting the log $\tau(T)$ vs $1/T$ line obtained from the experimental data with an appropriate equation (e.g., eq 5). This procedure, which is often referred as the Bucci method, is used in the analysis of peaks for electrets at which the depolarization follows a Debye-like exponential decay (eq 2).

Deviations in the shape of a TSDC peak from that described by eq 6 are interpreted on the basis of discrete or continuous distributions in the relaxation times $\tau(T)$. For mechanisms presenting a distribution of the activation energies $G(E_{\mathrm{a},i})$, and using eq 5, the TSDC signal can be expressed as

$$j(T) = \frac{P_0}{\tau_0}\sum_i G(E_{\mathrm{a},i})\exp\left[-\frac{E_{\mathrm{a},i}}{k_\beta T} - \frac{1}{b\tau_0}\int_{T_0}^{T}\exp\left(-\frac{E_{\mathrm{a},i}}{k_\beta T}\right)\mathrm{d}T\right]\Delta E_{\mathrm{a},i} \tag{8}$$

For DRS measurements disklike specimens were sandwiched between gold-coated brass electrodes, and the complex dielectric permittivity, ϵ^* , was determined as a function of frequency (10^{-3}−10^7 Hz) at selected temperatures between 300 and 413 K (controlled to better than ±0.1 K). A Schlumberger frequency response analyzer (FRA SI 1260) supplemented by a buffer amplifier of variable gain (Chelsea dielectric interface) was used for the room temperature (RT) frequency scans. A Hewlett-Packard 4284A precision RLC meter was used in combination with the Novocontrol Quatro Cryosystem for the measurements above RT. The TSDC scans covered the range 40−320 K and were performed in a vacuum between 10^{-1} and 10^{-4} Pa. The global current thermograms were obtained with the following experimental parameters: $T_\mathrm{p} = 320$ K, $E_\mathrm{p} \approx 2 \times 10^6$ V/m, $t_\mathrm{p} = 5$ min, and $b = 5$ K/min. Samples of typical dimensions ($5 \times 5 \times 1$) mm^3 were used. Prior to the measurements, both surfaces of the samples were cleaned with CCl_4. The TSDC experimental apparatus is described elsewhere.[35]

3. Results

The mechanical and dielectric relaxation behavior of poly(methyl methacrylate) is adequately documented.[45,47−49] A series of well-established intrinsic relaxation signals, denoted γ, β, α, and ρ in order of increasing temperature in the $I(T)$ scans and decreasing relaxation frequency (f_m) in the dielectric loss $\epsilon''(f)$ spectra, are representative of the various types of short-range and long-range segmental mobilities in PMMA.[45,47,49]

The γ relaxation signal is attributed to the α-methyl groups, i.e., methyls covalently bonded to the macromolecular chain.[47] Because of the low polarity of the $-CH_3$ group, the γ dielectric signal is very weak. The dominant signal of the secondary (β) relaxation mode presents at TSDC maximum T_β around 230 K (for atactic specimens) and involves localized conformational changes that require motion about only one or two bonds. As a rule, this relaxation is assigned to the motion of the carboxymethyl ($-COOCH_3$) side group, which is believed to involve a transition from an equilibrium position to another about the carbon−carbon bond linking the side group to the main chain.[50]

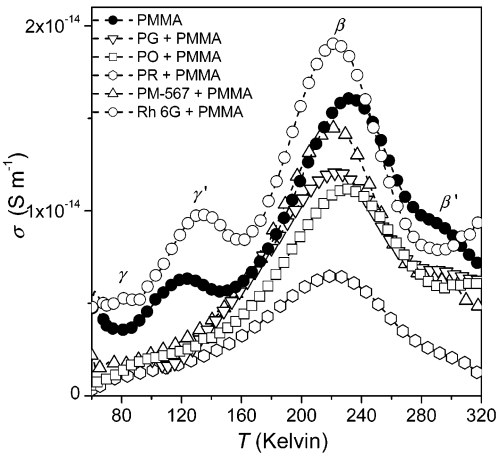

Figure 2. Thermally stimulated depolarization transient conductivity [$\sigma(T)$] spectra of undoped PMMA and its mixtures with the fluorescent dyes PG, PO, PR, PM-567, and Rh 6G.

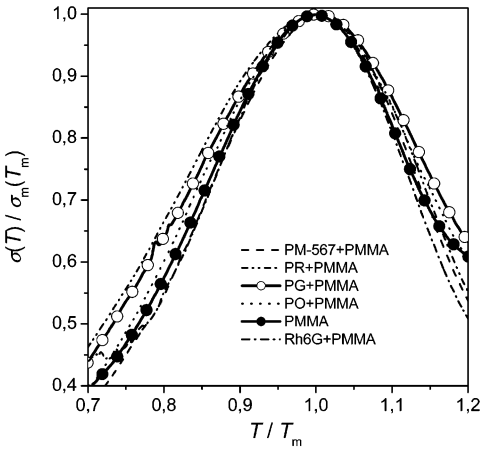

Figure 3. Reduced spectra of the transient conductivity ($\sigma(T)/\sigma_m(T_m)$ vs T/T_m) for the β relaxation signal of undoped PMMA and mixtures of PMMA with PG, PO, PR, PM-567, and Rh 6G.

The number of side groups for which rotation is possible essentially determines the intensity of the β relaxation signal. To a lower extent, the mechanism is influenced by the magnitude of the steric hindrances exerted on the ester groups by neighboring α-methyls or by extrinsic molecular species residing in the vicinity of the side group. The glass-to-rubber transition (α) process (at T_g, with TSDC maximum T_α around 378 K for atactic PMMA) is ascribed to a long-range conformational change of the polymer backbone with cooperative motions involving between 8 and 20 bonds. At temperatures near and above T_g, the reduced viscosity of the amorphous polymer facilitates the translational mobility of space charges and produces the ρ peak.

Figure 2 shows the reduced TSDC spectra of PMMA and its blends with the luminescent dyes PG, PO, PR, PM-567, and Rh 6G (Figure 1). For easier comparison between samples of different dimensions the as-received current (I) vs temperature (T) spectra are converted to (transient) conductivity σ units ($\sigma(T) = I(T)/E_pS$, where S is the cross-sectional area of the sample). In all dye + PMMA blends presented in Figure 2, the general structure of the TSDC spectrum of PMMA is retained. The β relaxation signal extends over a broad temperature range and in undoped PMMA presents a peak maximum at $T_\beta = 232.7 \pm 0.5$ K. In the presence of the dyes the secondary relaxation signal presents a moderate downshift that depends on the molecular structure of each dye. In decreasing order, the observed T_β values are as follows: 230.5 ± 0.5 K (PO + PMMA), 223.5 ± 0.5 K (PR + PMMA), 222.5 ± 0.5 K (Rh 6G + PMMA), 222.0 ± 0.5 K (PG + PMMA), and 219.9 ± 0.5 K (PM-567 + PMMA).

The relatively weak signals in the low-temperature (low-T) side of the β bands, between ∼100 and 160 K, are ascribed to a rotational relaxation mode from polar water molecules adsorbed in the polymeric phase (γ' mode).[34,46,47] The variation in their strength reflects the difference in the initial amount of water adsorbed in each sample as a result of the variations in the sample preparation processes and the storage conditions. The enhanced intensity and the drastic high-temperature (high-T) shift of the γ' signal in Rh 6G + PMMA is most probably related to the traces of the polar EtOH solvent. Below ∼100 K, the TSDC spectra demonstrate part of the signal arising from the weak (dielectrically) γ relaxation mode ($T_\gamma \approx 80$ K).

The α transition TSDC signal of PMMA with high syndio content (present case) is expected to peak at a temperature $T_\alpha \approx T_g$, between 378 K (atactic PMMA) and ∼400 K (syndiotactic PMMA). Note that the amount of water adsorbed in room-stored PMMA is typically around 0.6% of the dried material and a lowering of T_g by approximately 1 deg per 0.1% of weight increase due to hydration is expected.[51] Moreover, irrespective of the plasticizing influence of the chromophores[36,39,40] to the micro-Brownian motion of the chain segments, the downshift of T_α is not expected to exceed 40 K. For example, differential scanning calorimetry (DSC) studies in several dye + PMMA blends give $\Delta T_g \leq \pm 7$ K for perylene ($R_1 = R_2 = H$),[39] −17 K for 3-(1,1-dicyanoethenyl)-1-phenyl-4,5-dihydro-1*H*-pyrazole,[52] ≈−25 K for *N*,*N*-dimethyl-*p*-nitroaniline,[41] and ≤−34 K for 4-[ethyl-(2-hydroxyethyl)amino]-4′-nitroazobenzene.[40] In view of the above considerations, the α signal is anticipated outside the investigated temperature range, in line with the spectra shown in Figure 2. The bend in the high-T side of the β signal of PMMA is tentatively attributed to the controversial β' relaxation signal.[53]

The TSDC signal of the secondary relaxation mode is symmetrically broadened in the PG and PO + PMMA blends (Figure 3), while in PR + PMMA it is broader only at its low-T side. In PM-567 + PMMA the width of the β band does not show any significant variation, while in the Rh 6G + PMMA blend the signal appears slightly narrower. The observed variations may be considered blending effects on the relaxation characteristics of the side-chain mechanism and not artifacts arising from contributions of satellite relaxation modes. For example, the water-related γ' relaxation mode activates below approximately 0.70 T/T_β, while the low-T tail of the primary α transition signal (from isotactic sequences of PMMA) is expected above about 1.25 T/T_β.

According to Starkweather,[54,55] the secondary relaxation of PMMA is a noncooperative relaxation process, and a broad distribution in the activation energies has to be invoked for the explanation of its non-Debye character in dielectric experiments. The potential barrier to the rotational mechanism of the ester carbonyl side groups has a specific intramolecular part,[47,56] and the distribution is related to intermolecular interactions that influence to the rotational motion. In the present case, for the decomposition of the broad β-relaxation

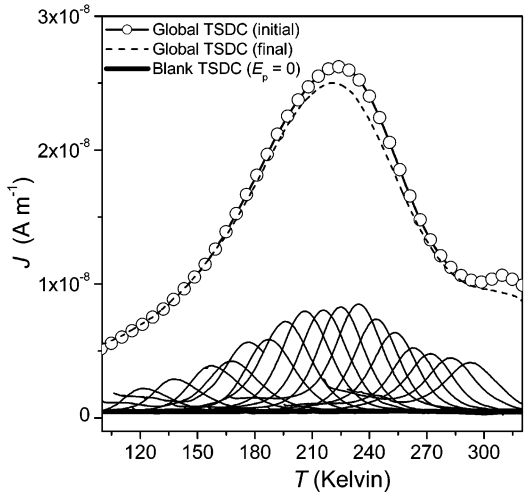

Figure 4. Global TSDC thermograms obtained for perylimide red + PMMA and the FP responses isolated in the region of the β relaxation. The spectra recorded before and after the completion of the FP scans are given for comparison.

signal we have employed the fractional polarization (FP) technique. This technique consists of "sampling" the relaxation process within a narrow temperature range by polarizing at a temperature T_p and depolarizing at T_d a few degrees lower than T_p and by spanning the entire temperature range of the global peak with a series of FP measurements. This thermal cycling is not expected to have any influence on the form of the distribution in the case of local relaxations. On the other hand, the analysis of the FP responses results in an easier interpretation of the peaks as the current "samples" are quasi-nondistributed. In Figure 4 we show, as a representative example, the FP peaks obtained for the PR + PMMA blend. The characteristic parameters (E_a, τ_0) of each fractional polarization band have been determined using typical curve-fitting procedures described elsewhere.[57]

With FP the distributed polarization is investigated in parts: in the low-T polarization windows the fast groups of the polar carboxymethyl pendant groups are oriented and subsequently (re)oriented to produce the FP band. By increasing T_p, the slower and highly constrained dipoles gain enough mobility to (re)orient. Figure 5 presents, as representative examples, the normalized curves for the FP bands in the range of the β signal, recorded for PO + PMMA (Figure 5a) and PG + PMMA (Figure 5b). The FP spectra become narrower as the T_p increases, behavior typical of activation energy-distributed relaxation mechanisms. The narrowing is more intense for the PO + PMMA mixture, indicative of a sharper increase of E_a with temperature (see data in Figure 6).

Figure 6 shows the variation of the apparent activation energy barriers E_a as a function of T_p for the entire range of the investigated materials. The distribution presents the lowest energy barriers for undoped PMMA and PG + PMMA and is drastically elevated for the other blends with PM-567 + PMMA presenting the most significant increase. Note that the energy upshifts are higher than the least-squares line-fitting errors, which are comparable to the natural incertitude interval $\Delta E_a \cong k_\beta T_m$ (thermal energy factor $k_\beta T_m$).[58] The similarity in the energy spectra of PMMA and PG + PMMA agrees well with the conclusions from previously reported partial heating data.[34,35] For some of the materials,

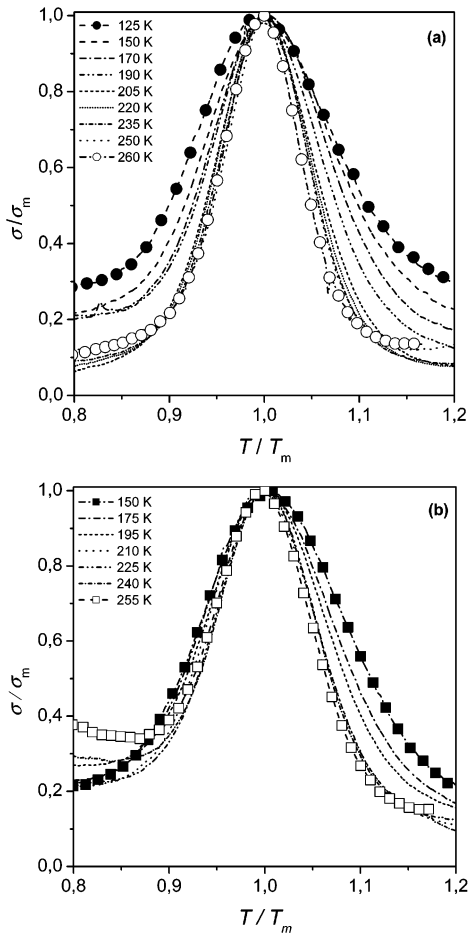

Figure 5. Normalized transient conductivity curves (σ/σ_m vs T/T_m) of the fractional polarization bands recorded for (a) perylimide orange + PMMA and (b) perylene green + PMMA.

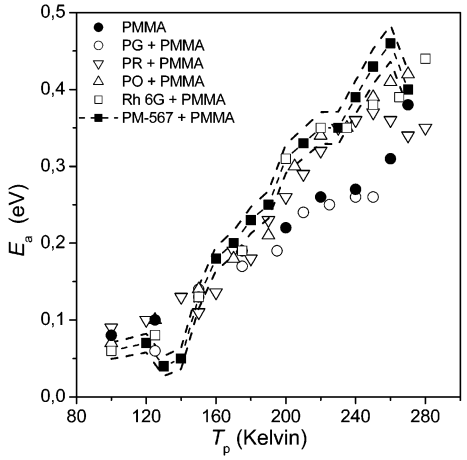

Figure 6. Plot of the apparent activation energy barriers, E_a, as a function of the polarization temperature, T_p, recorded for undoped PMMA and the dye + PMMA mixtures. For PM-567 + PMMA we present the natural incertitude interval $E_a \pm k_\beta T_m$ (dashed lines) as a measure of the errors in the estimation of E_a.

strong deviations from the nearly linear behavior of the $E_a(T_p)$ variation are attributed to current signals from neighboring polarization modes, e.g., from adsorbed water molecules (below ~150 K) and the β' mechanism (above ~260 K).

With respect to the analysis of the broad β bands with fractional polarization, two general observations must

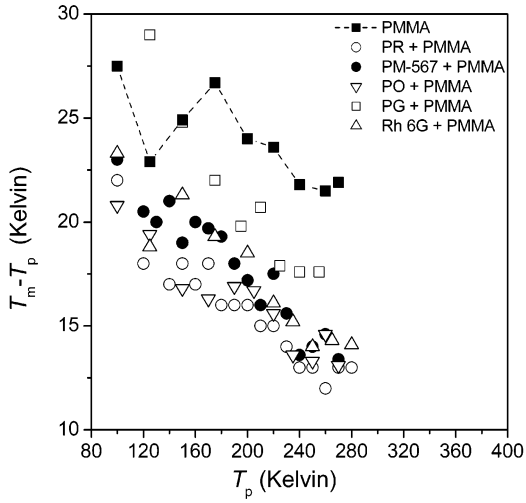

Figure 7. Plot of the $T_m - T_p$ vs T_p dependences obtained with use of the fractional polarization TSDC technique for undoped PMMA and its mixtures with PG, PO, PR, PM-567, and Rh 6G.

be pointed out. The first observation is the demonstration of a linear relationship between log τ_0 and E_a of the type

$$\log \tau_0 = \log \tau_c - \frac{E_a}{\ln(10) k_\beta T_c} \tag{9}$$

for some of the materials studied with the FP technique. This dependence, known as a compensation law, has been observed for α transitions in polymers and correlates the compensation temperature T_c with the glass transition or the fictive equilibrium temperatures. Nevertheless, the observation of a compensation effect for the local noncooperative β relaxation of PMMA[34,35] has no physical meaning. A relation between E_a and τ_0 is already expected due to the equation

$$\tau_0 = \frac{k_\beta T_m^{\,2}}{b E_a} \exp\left(-\frac{E_a}{k_\beta T_m}\right) \tag{10}$$

which is valid for any TSDC peak. We demonstrated[59] that a compensation effect could not be observed for a material for which the activation energy is a linear increasing function of temperature, as it is approximately the case with the data in Figure 6.

The difference between the temperature of maximum intensity of an elemental peak T_m and the polarization temperature T_p is considered to provide information about the contribution of the molecular mobility to the dielectric relaxation.[60] In Figure 7 we present the $T_m - T_p$ vs T_p dependences observed for undoped PMMA and its dye blends. In most cases there appears to be a decreasing trend in the $T_m - T_p$ vs T_p variation in the range of the local β relaxation. In a recent report the fractional polarization TSDC technique was used to analyze the shift of the peak position in the temperature range of the glass transition of the amorphous phase for poly(ethylene terephthalate) (PET).[60] It has been proposed that the dielectric transition temperature associated with the nonlocal α relaxation may be determined from the condition $T_m - T_p = 0$. At $T_m = T_p$ the dipoles move equally fast during polarization or the depolarization stage. By considering the β relaxation of PMMA as the precursor of the large-scale conformational motions of the polymer backbone around T_g, it would appear reasonable to attempt an indirect estimation of $T_{g,diel}$ from the above plot using the condition $T_m = T_p \approx T_g$. In all cases the linear fits of the data in the region of the secondary signal give unrealistic values (442 K < "T_g" < 536 K, with error ≥ ±20 K). For example, in PR + PMMA with the most isolated TSDC β signal, we estimate a "T_g" value of 469 ± 23 K. A plausible reason for the failure could be the presence of relaxations that superimpose with the response of the β relaxation (e.g., see the enormous changes of the data for PMMA; Figure 7).

In the dielectric loss $\epsilon''(f)$ spectra the α and β relaxation processes occur independently at atmospheric pressure and $T \leq 1.2T_g$, while for temperatures more than $1.2T_g$ the two processes merge (or are coupled) into a single process referred to as $\alpha\beta$.[56] In the present DRS study we performed isothermal frequency scans at temperatures between 300 K (RT) and 413 K ($\sim 1.1T_g$ assuming that T_g = 378 K for amorphous PMMA). Accordingly, the signal of the β relaxation mechanism was well separated from the α transition losses. Note that priority in the comparison and the evaluation of the DRS data must be given to the low-T measurements. In some of the blends, uncontrolled thermally initiated reactions between the dye molecules and their polymeric environment may obscure the correct assessment of the effects of blending on the rotational relaxation dynamics of the ester carbonyl side groups.

Figure 8 shows the frequency dependences of the dielectric permittivities ϵ' (Figure 8a) and the dielectric loss factors ϵ'' (Figure 8b) of undoped PMMA and of the dye + PMMA blends, recorded at 300 K. A common feature in these spectra is the intense relaxation signal associated with the β relaxation mode with loss maxima, f_m, between 1 and 10 Hz (Table 1). At RT the α transition activates below ca. 10^{-5} Hz. In addition, the low-T TSDC mechanisms (below the β band, Figure 2) are expected to produce weak loss peaks at the high-frequency (high-f) limit of the investigated spectrum (in the MHz−GHz region for scans performed near RT). In some cases, the spectrum in the low-frequency (low-f) range 10^{-3}−10^{-1} Hz presents relatively intense losses that are most likely mainly due to a conductivity mechanism. A successful fitting of the total $\epsilon''(f)$ spectrum of perylimide red + PMMA, with a superposition of a conductivity term (low-f range) and a HN function (eq 4, for i = 1), is shown in Figure 9.

Figure 10 shows the variation of the $\epsilon''(f)$ spectrum of PMMA and PR + PMMA with temperature. For clarity, the original spectra and the HN simulations only at the extreme temperatures are presented. In Table 1 we summarize data deriving from the analysis of the secondary dielectric relaxation loss bands recorded at 300 and 413 K. The parameters of the Havriliak−Negami equation ($1 - \alpha_{HN}$, β_{HN}, f_m, and $\Delta\epsilon$) for the β relaxation recorded in undoped PMMA and the various dye + PMMA mixtures are presented. As expected, by increasing the temperature the loss band shifts to higher frequencies, the dielectric strength increases (i.e., higher $\Delta\epsilon$) and the distribution of the relaxation times decreases (i.e., $1 - \alpha_{HN}$ decreases).

Figure 11 compares the characteristic apparent activation energy parameters for the secondary relaxation signals recorded from thermostimulated depolarization currents and dielectric relaxation spectroscopy. A de-

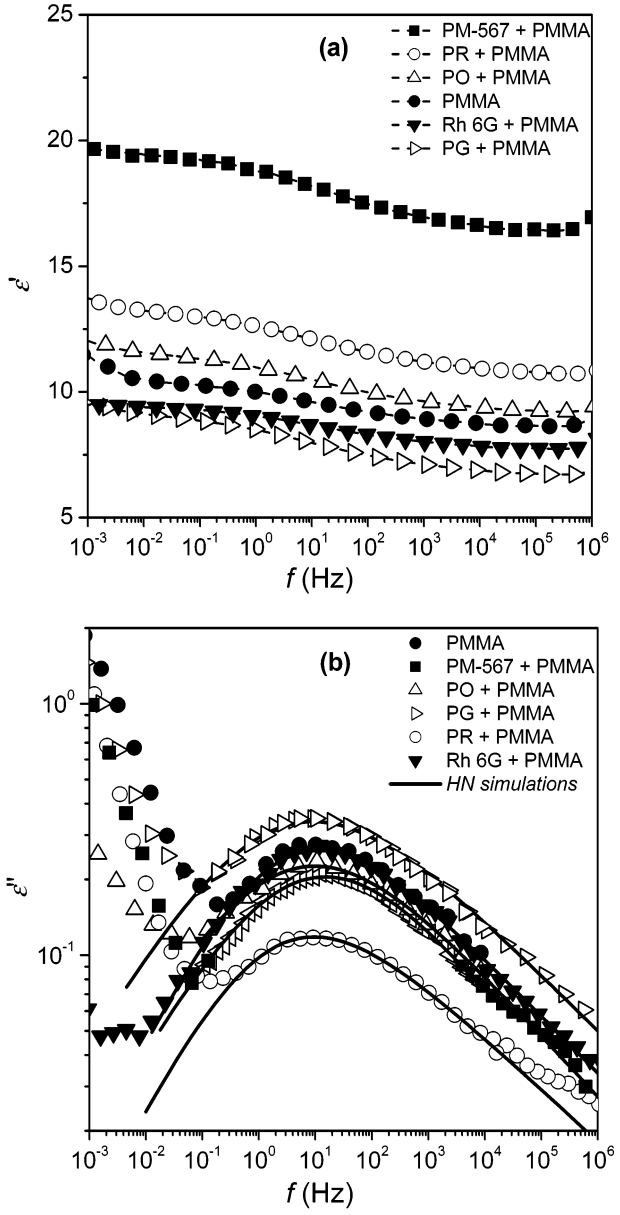

Figure 8. Frequency dependence of dielectric permittivities (a) and dielectric losses (b) of undoped PMMA and mixtures of PMMA with PG, PO, PR, PM-567, and Rh 6G. Spectra recorded at RT and atmospheric pressure.

tailed discussion of the presented behavior will be attempted in the following section. The energies deriving from the TSDC study are representative of the β mode (E_a value at $T = T_m$, Figure 6). The DRS activation energy of 0.88 ± 0.03 eV calculated for undoped PMMA agrees well with former DRS results.[39,61] The apparent energy barriers determined for the β relaxation mechanism of PMMA by means of TSDC, DRS, and dynamic mechanical spectroscopy (DMS) methods present a large scattering.[61] In addition, the E_a values generally obey the relation $E_{a(TSDC)} < E_{a(DMS)} < E_{a(DRS)}$, consistent with the results presented in Figure 11. This dependence is most likely related to the different modes of molecular diffusion that are coupled by the mechanical or electrical perturbation stresses.

Figure 12 compares the relaxation strength of the β relaxation signals recorded by DRS ($\Delta\epsilon$ at 300 K) and TSDC. In the latter case, the relaxation strength $\Delta\epsilon$ (at $T \approx T_p$) is calculated from the depolarization charge Q, obtained from the area under the TSDC β peak, by

$$\Delta\epsilon = \frac{Q}{S\epsilon_0 E_p} \tag{11}$$

The errors in this estimation are expected to account to ±10% of the actual $\Delta\epsilon$ value (error bars for TSDC data) due to the strong overlap of the secondary peak with other signals and some uncertainty in the subtraction of the background current. For the DRS values the error is considerably lower (less than ±5%). The agreement of the $\Delta\epsilon$ variations for the entire range of the investigated materials confirms the complementary nature of the two methods; however, the exact values of the temperature-dependent parameter $\Delta\epsilon$ as they derive from the nonisothermal TSDC study may be treated with cautiousness. For example, since $T_p > 300$ K, one should expect the $\Delta\epsilon$ values determined by TSDC to be slightly higher compared to those determined by DRS.

4. Discussion

4.1. Photophysical Characteristics and Sub-Glassy Dielectric Response of the Polymer-Based SSDLs. In general, the photophysical characteristics of the trapped dye molecules are influenced by a number of parameters. The principal factor is the degree and the type of intermolecular and intramolecular interactions between the dye and surrounding chemically active molecules (e.g., end groups, adsorbed O_2, unreacted monomers, initiator radicals, and additives). Of special significance is the strength of the coupling interactions between the dye molecule and polymer segments. An additional factor is the available free space around the dye molecule, i.e., the size of the dye relative to the average size of the caging environment provided by the polymer matrix. The latter controls the mobility of the dye molecule and influences the rates of the nonradiative processes in the SSDL matrices. Energy-transfer processes and charge-transfer interactions between the dye and the matrix as well as among dyes (in multidoped polymer blends such as Rh 6G:Rh B + PMMA[62]) are also of great importance.

With respect to the dielectric behavior of the SSDLs, the above factors are expected to have an effect on the side-chain and the segmental mobilities of the polymer host. The combination of thermally stimulated depolarization currents and dielectric relaxation spectroscopy revealed several modifications of the β relaxation dynamics produced by the dye molecules. A major effect of blending is designated by the modification of the spectrum of the energy barriers associated with the side-chain (re)orientation process (Figures 6 and 11) and some changes in the width and the asymmetry of the signal (Figure 3 and Table 1). Second, an appreciable speed-up of the conventional β relaxation mode is recorded in all dye + PMMA blends. This effect is clearly exemplified by the low-T shift of the β thermocurrent bands (Figure 2) and the high-f shift of the ϵ'' signals (Table 1). Changes in the contribution of the β mechanism to the static dielectric permittivity of the polymer structure (Figure 12) are also indicative of selective plasticization and antiplasticization effects.

4.2. Effects of the Apolar and Neutral Dyes on the β Relaxation Mode of PMMA. Incorporation of perylene green in PMMA causes a moderate decrease in the height of the distributed activation energies, near

Table 1. Parameters of the Havriliak−Negami Equation (f_m, α_{HN}, β_{HN}, and $\Delta\epsilon$) for the β Relaxation Signals Recorded in Undoped PMMA and the Various Dye + PMMA Mixtures

	T (K)	PMMA	PG + PMMA	PO + PMMA	PR + PMMA	PM + PMMA	Rh6G + PMMA
$1 - \alpha_{HN}$	300	0.51	0.62	0.61	0.56	0.60	0.55
	413	0.49	0.44	0.39	0.40	0.44	0.38
β_{HN}	300	0.44	0.59	0.63	0.54	0.71	0.51
	413	0.98	0.62	0.57	0.51	0.90	0.66
f_m (Hz)	300	1.57	2.42	3.13	2.10	6.61	2.69
	413	96000	27000	59000	24000	132000	112000
$\Delta\epsilon$	300	1.98	2.69	1.68	0.90	1.43	1.84
	413	3.31	4.17	3.40	1.54	1.70	3.32

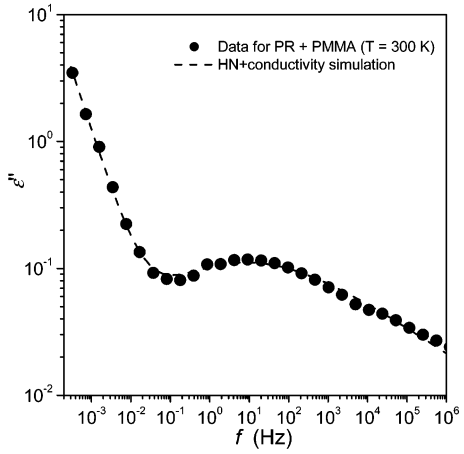

Figure 9. Fitting of the loss spectrum of the PR + PMMA blend. Spectrum recorded at RT and atmospheric pressure. The HN parameters for the β relaxation are given in Table 1.

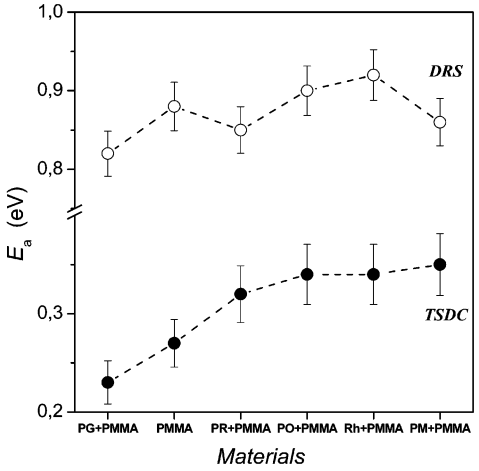

Figure 11. Plot of the variation of the apparent activation energy parameters E_a of the secondary relaxation calculated from the two dielectric methods.

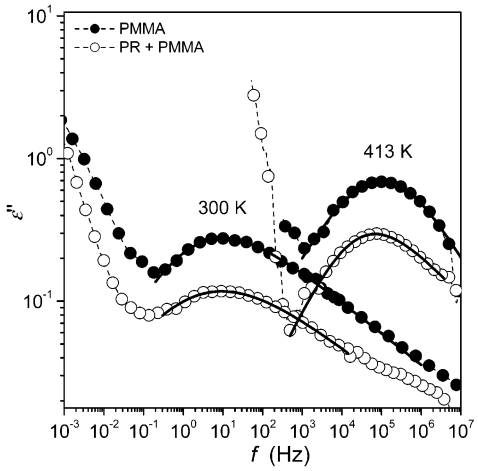

Figure 10. Change of the $\epsilon''(f)$ spectrum of PMMA and PR + PMMA with increase of temperature from 300 to 413 K. The HN simulations of the β loss signals are also presented.

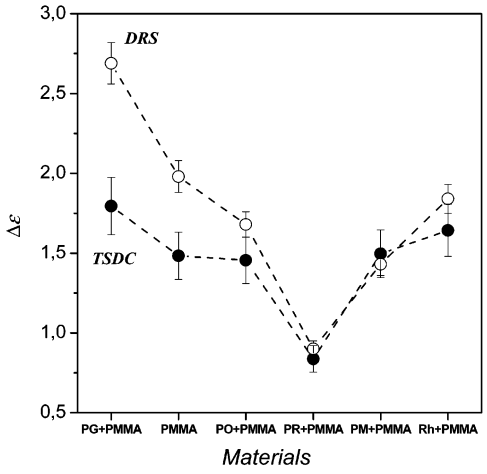

Figure 12. Plot of dielectric strength of the secondary relaxation signals ($\Delta\epsilon$) determined by means of DRS (at 300 K) and TSDC (at $T \approx T_p$).

the limit of the experimental error, and a substantial low-T shift of the TSDC band or, equivalently, a high-f shift of the DRS loss band. Both changes indicate that the guest molecules facilitate the side-chain relaxation mode of the polymeric host. The width $1 - \alpha_{HN}$ (0.62, at 300 K) and the asymmetry β_{HN} (0.59, at 300 K) of the β relaxation in PG + PMMA are higher relative to their values in undoped PMMA (0.51 and 0.44, respectively). $\Delta\epsilon$ rises drastically from 1.98, in undoped PMMA, to 2.69 in the PG + PMMA mixture (Figure 12), and that despite the fact that the number of the pendant groups is expected to present a slight decrease due to the addition of the dye. Similar effects can also be observed in the TSDC study (see Figures 3 and 12). The change in $\Delta\epsilon$ suggests a drastic plasticization of the β mode, i.e., enhancement of the mobility of the carboxymethyl side groups of the host polymer, probably due to an increase in the free space.[36] Experimental evidence for enhanced lasing action of various perylenes in PMMA + based matrixes[10,63] is in good agreement with the present comparative ac/dc dielectric results and earlier TSDC studies,[34,35,38] which demonstrate weak, if any, interactions of the side chains with the PG molecules.

More information can be drawn from the dielectric data by comparing the results for the PG + PMMA mixture with those obtained for the bulkier substituted perylimide + PMMA solid solutions. The dissimilarities between PG and the perylimide derivatives, related to the chemical structure and the size of the molecule, are

expected to affect differently the β relaxation dynamics. Perylimide orange is an efficient dye with a fluorescence quantum yield of nearly 1 in cyclohexane. It is liable to dye aggregation and exhibits solvatochromic properties. PO has slightly larger length (~10% longer) and four carbonyl groups per molecule, compared to the two carbonyl groups per molecule of PG. The latter group shows the highest tendency for hydrogen-bonding interaction with acidic groups.[34,35] Perylimide red has a fluorescent quantum yield of 0.93 in composite SiO_2 + PMMA matrices and is reported to be extremely photostable.[10] Relative to the orange chromophore, perylimide red is substantially larger (~ 50% thicker). In both perylimides the carbonyls are positioned at the phenyl rings in the main body of the molecule, thus less mobile, and probably effectively screened by the bulky alkyl-substituted phenyl rings (and the additional alkyl side groups in PR), compared to the PG molecule.

At variance with PG, the presence of perylimide orange clearly increases the energy barriers of the β relaxation process (Figure 11) with a moderate antiplasticizing effect (~15% decrease in $\Delta\epsilon$, from 1.98 to 1.68 at 300 K, Figure 12). The rise of the E_a spectrum is drastically intensified compared to the variation determined by means of the partial heating method in earlier TSDC studies of PO + PMMA.[34,38] The present observations seem to be in agreement with the DRS results of El-Shaarawy et al.[39] for a dye + PMMA mixture (perylene dye with $R_1 = R_2 = -H$, molecular weight 252.32 g mol^{-1}).

Substitution of PO by the bulkier perylimide red dye, at the same concentration, has no additional effect on the activation energy spectrum (Figure 6), but the strength of the secondary dielectric relaxation signal drastically reduces by ~55% (from 1.98 in undoped PMMA to 0.90 in PR + PMMA, at 300 K, Figure 12). These observations suggest that the interchange of the perylimide chromophores principally influences the free space in the polymer matrix; an increase of the ratio of the size of the dye relative to the average size of the caging environment is anticipated. In view of that, less free space is expected around the carboxymethyl side groups. Therefore, owing to increased steric hindrances and possibly some additional intermolecular interactions due to the reduced intermolecular distances, the behavior of the perylimide dye blends is clearly differentiated compare to PG + PMMA. Conversely, the dye is expected to face more restricted caging environment, which should result to reduced rotational and translational mobilities. The latter is in agreement with recent optical studies for substituted perylene and perylimide derivatives: strong fluorescence and better photostabilities have been reported for PO and PR in PMMA and SiO_2 + PMMA compared to organic solutions or the inorganic SiO_2 glass carriers.[10,63]

We should note that the validity of any conclusion deriving from the above comparisons rests on the use of similar dye concentrations. This condition is fulfilled in the present study, where $C \approx 10^{-4}$ mol/L for all substituted perylene SSDLs. Wide variations of C can modify polymer's response in distinctly different directions. For example, for low dye contents the dye may simply fill voids in the polymer structure, without intense effects on the intrinsic relaxation modes, while at higher concentrations the dye may restrict the rearrangement of the local and/or the long-range structure.[39]

An intriguing result is the observation of a downshift of T_β, despite the elevation of the E_a distribution. This effect is more pronounced for the perylimide orange + PMMA blend. On the basis of the transcendental eq 10 that interrelates the relaxation parameters of the mechanism (τ_0, T_m, and E_a), a decrease in T_m accompanied by an increase in E_a necessitates a drastic decrease in the preexponential factor of the Arrhenius equation (eq 5). This suggests an increase of the jump frequencies or more precisely the frequency of the 180 ± 20° flip motion of the OCO plane of the side group between two potential energy minima.[50] In the equivalent Arrhenius and Eyring−Kauzmann formulations for $\tau(T)$, a drop in $\tau_0 \propto \exp(-\Delta S/R)$, R being the gas constant, is consistent with an increase of the activation entropy factor ΔS. The latter changes are indicative of a short-range deformation of the "lattice" (i.e., configurational changes of the macromolecular structure) in the proximity of the side groups due to the presence of the dye.

4.3. Effects of the Polar and Ionic Dyes on the β Relaxation Mode of PMMA. A more complex and obviously more interesting dielectric response characterizes the mixtures of PMMA with the polar/ionic dyes. An additional differentiation of the Rh 6G/PM-567 + PMMA solid solutions from the previous blends is the use of ethyl alcohol in the SSDL matrices, traces of which are expected to exist in the tested samples. Ethanol is essential for the dissolution of polar dyes in nonpolar MMA. Moreover, it has been found that alcohol-modified PMMA presents improved optical response (e.g., enhancement of host laser damage[5]).

Relative to undoped PMMA and the perylene and perylimide dye + PMMA mixtures, the blends with PM-567 and Rh 6G chloride show the higher increase in the E_a spectrum (TSDC data, Figures 6 and 11). The discrepancy between the DRS- and TSDC-derived activation energy parameters for PM-567 + PMMA (Figure 11) is most probably related to the partial degradation of the dye during the high-T frequency scans. The pyrromethene−BF_2 complexes are unstable; yet, because of their high efficiency, they present good prospects for longer pulse length operation especially in deoxygenated systems.[64] Because of the presence of an aromatic amine group in its structure, PM-567 is vulnerable to photodegradation due to photochemical reactions with singlet-state oxygen. Dissolved oxygen is already present in MMA and PMMA. Additional oxygen can be produced by thermally initiated reactions and in combination with thermally liberated electric charges (e.g., electrons) may contribute to a substantial deactivation of the dye. For example, during the high-T DRS scans, the small amount of unconverted monomers and initiator radicals in PMMA is expected to gain enough mobility and participate in free-radical chemical polymerization reactions that produce oxygen.[65]

Consonant with the preceding analysis is the observation that PM-567 + PMMA presents the lowest value for the percentage increase of $\Delta\epsilon$ for the β relaxation mode in going from room temperature to 413 K (Table 1). The increase is only +18.9% for PM-567 + PMMA compared to the +55.0% for PG + PMMA, +67.2% for undoped PMMA, +71.1% in PMMA with PR, +80.4% for the Rh 6G, and +102.4% for the PO + PMMA blends. This can be explained if we consider that some products of the thermally produced chemical modification of pyrromethene 567 present strong interactions with the

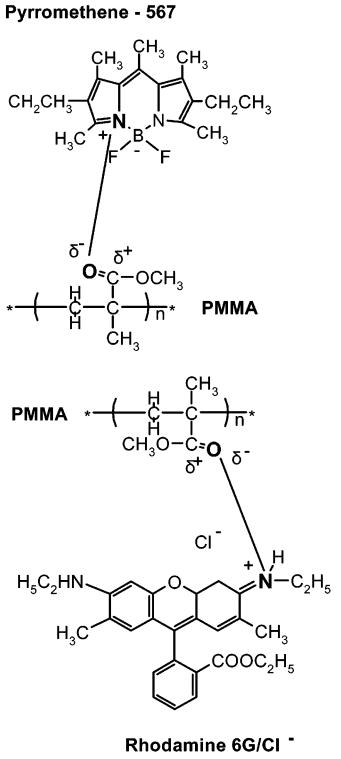

Figure 13. Dipole−dipole interaction between side chains of PMMA and the highly polar and ionic dyes PM-567 and Rh 6G. Electrostatic interactions between B^- (in pyrromethene−BF_2) or Cl^- (in the xanthene compound) and the carbon atom (δ^+) of the side group are also possible.

ester carbonyl groups and quench their rotational mobility.

From the data shown in Figure 3 and in Table 1 it appears that the TSDC and the DRS signals of the β relaxation mechanism in Rh 6G + PMMA are narrower, i.e., closer to the Debye-type response, compared with the same signal in undoped PMMA. This indicates that the ester carbonyl groups of PMMA face a less heterogeneous microenvironment. This may be related to the relatively small size of the Rh 6G and PM-567 dye molecules and their increased ability to penetrate smaller voids in the macromolecular structure. Moreover, the intense apparent activation energy upshifts may be primarily related to the broader range of interactions between the side groups of PMMA and the confined dyes, e.g., intermolecular dipole−dipole type interactions (Figure 13) and electrostatic interactions with the positively charged xanthene chromophore and the negatively charged counterion (Cl^-). Both dye + PMMA blends present the most extreme changes: the highest downshift of the TSDC β band and the stronger upshift of the E_a spectrum. Unexpectedly, while the side groups strongly interact and are possibly drastically sterically hindered by the polar/ionic dye molecules they acquire increased relaxation frequencies.

Note that the polymerization of the monomer−initiator mixture in the presence of the dyes, and especially of the highly ionic and polar xanthene and pyrromethene−BF_2 types and their solvent ethanol, may be responsible for severe changes in the long-range conformation of the macromolecules (i.e., their length, packing, and interconnection). This issue cannot be analyzed at the present stage. An answer is expected to emerge from studies of the dielectric and thermal α transition signals in the dye + PMMA blends (study in progress). Recent DSC estimations of T_g for radical polymerized perylene + PMMA mixtures revealed a moderate increase of the glass-to-rubber transition temperature up to a certain value of the dye concentration and decrease for higher dye loadings.[39] The peculiar dependence of T_g from the dye concentration has been assigned to irregular variations of the polymeric free volume.

4.4. Connection between Lasing Characteristics and Dielectric Response: Comments on the Rh6G/Cl^- + PMMA System. It would be interesting to attempt to correlate some observations of the present dielectric spectroscopy study with an intriguing topic in optical applications, i.e., the dependence of the efficiency and photostability of the dyes from the provided caging environment. The following comments address issues mainly related to the optical response of rhodamine 6G, a point of reference for all dye molecules.

It has been already stated that the enhancement of the structural mobility of the chromophore in a given medium is expected to decrease its fluorescence efficiency. In most cases the low photostability and efficiency of Rh 6G/Cl^- in the presence of PMMA as surrounding medium has been attributed either to the nonpolar nature[2,21] or to the relatively high flexibility[66,67] of the macromolecular environment. The first explanation is easily comprehensible. In typical nonpolar media (e.g., chloroform and PMMA) the chloride ion is not fully dissociated and excited-state charge-transfer interactions between the cationic dye molecules, and the anions cause deactivation of the chromophores. Accordingly, the introduction of polar low molecular weight additives (e.g., ethanol, EtOH), which enhance the microscopic dielectric constant around the dye, facilitates the formation of expanded ionic pairs and improves several optical characteristics of the PMMA-based SSDLs. For example, polymerization causes a decrease in the dielectric constant ($\epsilon_{MMA} = 4$, $\epsilon_{PMMA} \approx 2.9$), and this results in a shift of equilibrium between dye monomer molecules and their aggregates toward the latter.[68] The decrease in the dielectric constant of the medium causes the decrease of gain. Hence, the gain of the dye molecule in solid PMMA is lower than that in the liquid EtOH or MMA + EtOH media.

Nevertheless, the correlation of the lasing performance of dyes in PMMA with the matrix flexibility seems less straightforward. In going from the flexible polymer matrix to more rigid inorganic or composite glass environments, the dye mobility decreases and photostability/efficiency enhances;[9,10] yet, fluorescence efficiency remains clearly below the values attained at some liquid solutions of Rh 6G. In alcoholic solutions, for example, rhodamine 6G presents exceptional fluorescence quantum yields Q_f. $Q_f = 0.96$ in methanol (MeOH)[69] and reduces to 0.78 in PMMA.[17] This has been attributed to the fact that the carboxyphenyl constituent is held in a position nearly perpendicular to the xanthene dye by the bulky carbonyl group, thus allowing little, if any, mobility. In the excited state the π-electron density within the C=N bond is high, and the thermal energy of solvent molecules is considered insufficient to twist the amino groups out of planarity. For the above reason rhodamine 6G shows minimal benefit from the "rigidity" provided by the polymeric environment.[10] The absence of a distinct dielectric relaxation mode ascribed to the polar Rh 6G molecule indicates that caging in PMMA effectively reduces the rotational flexibility of

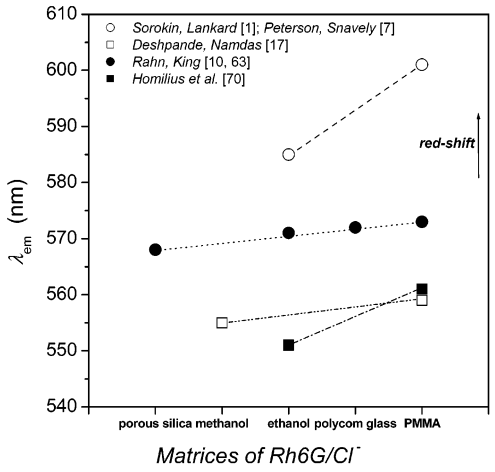

Figure 14. Dependence of the fluorescence emission maxima (λ_{em}) from the matrix incorporating the rhodamine 6G/Cl^- dye molecules.

the chromophore, at least at temperatures well below the glass-to-rubber transition temperature. On the other hand, if we consider the flexibility of the matrix as an inconsequential factor for the optical response of Rh 6G, and by virtue of the observed strong modifications of the β relaxation dynamics in Rh 6G + PMMA, it is reasonable to consider the occurrence of strong dye−host interactions as the origin of the deterioration in the optical response of this blend. Such interactions may produce the strong coupling between the side groups rotation and the rotations of the chromophores[41−43] and adversely change optical characteristics of the dye molecule. The strong red shift of the emission optical bands of Rh 6G in PMMA, compared to the bands in matrices of moderate (porous SiO_2, polycom glass) or high polarity (MeOH, EtOH), is a characteristic example (Figure 14). Coupling effects may also be invoked for explaning the low-T shift of the TSDC β band in Rh 6G + PMMA, dye-free PMMA + SiO_2, and the polycom Rh 6G + PMMA + SiO_2 matrix.[35]

5. Summary

The combination of isothermal dielectric relaxation spectroscopy and thermally stimulated depolarization currents revealed several modifications of the β relaxation dynamics of poly(methyl methacrylate) in solid solutions of various luminescent molecules (dye concentrations $\sim 10^{-4}$ mol/L).

Inclusion of the apolar and neutral perylene and perylimide molecules in PMMA primarily alters the free space of the polymer matrix. For perylene green, the local side-chain (re)orientation process of PMMA shows drastic plasticization effects. By increasing the size of the confined dye molecules (perylimides), the enhancement of the steric hindrances increases the apparent activation energy barriers and suppresses the strength of the dielectric β relaxation signals (antiplasticization effects). Reports of relatively good lasing performances in PMMA-based hosts, exhibited in particular by the high molecular weight perylimide dyes, are in accordance with the present results that demonstrate reduced rotational and translational mobility for the chromophores and weak intermolecular interactions in the polymeric cages of the dye molecules.

On the contrary, intense coupling of the (re)orientational motion of the carboxymethyl side groups of PMMA with the relatively low molecular weight and highly ionic and polar xanthene and pyrromethene−BF_2 type dyes is recorded. In their presence, the β process of the polymer matrix is drastically antiplasticized; the width of the distribution of the apparent activation energies compresses while their height shows an appreciable rise. On the basis of the present dielectric study, the relatively poor lasing performances of these dyes in PMMA hosts may be attributed to strong dipole−dipole and electrostatic interactions and charge-transfer processes between the dye molecules and their polymeric environment.

The study of the side-chain and the segmental mobilities in polar polymeric hosts, by means of DRS and TSDC, emerges as a useful spectroscopic approach for the characterization, the evaluation, and possibly the prediction of the lasing behavior of novel solid-state dye laser matrices.

Acknowledgment. Thanks are due to Dr. Mark D. Rahn (Laser Photonics Group, Physics & Astronomy Department, University of Manchester) for supplying the dye + polymer blends and for participating in valuable discussions.

References and Notes

(1) Sorokin, P. P.; Lankard, J. R. *IBM J. Res. Dev.* **1966**, *11*, 162.
(2) Drexhage, K. H. In *Dye Lasers*; Schäfer, F. P., Ed.; Topics in Applied Physics, Vol. 1, 3rd ed.; Springer: Berlin, 1990; pp 155−200.
(3) Stoilov, Y. Y. *Appl. Phys. B* **1984**, *33*, 63−74.
(4) Pavlopoulos, T. G. *Prog. Quantum Electron.* **2002**, *26*, 193−224.
(5) Singh, S.; Kanetkar, V. R.; Sridhar, G.; Muthuswamy, V.; Raja, K. *J. Lumin.* **2003**, *101*, 285−291.
(6) Soffer, B. H.; McFarland, B. B. *Appl. Phys. Lett.* **1967**, *10*, 266.
(7) Peterson, O. G.; Snavely, B. B. *Appl. Phys. Lett.* **1968**, *12*, 238.
(8) Hench, L. L.; West, J. K. *Chem. Rev.* **1990**, *90*, 33−72.
(9) Avnir, D.; Levy, D.; Reisfeld, R. *J. Phys. Chem.* **1984**, *88*, 5956−5959.
(10) Rahn, M. D.; King, T. A. *Appl. Opt.* **1995**, *34*, 8260−8271.
(11) Cazeca, M. J.; Jiang, X. L.; Kumar, J.; Tripathy, S. K. *Appl. Opt.* **1997**, *36*, 4965.
(12) Drabe, K. E.; Cnossen, G.; Wiersma, D. A. *Opt. Commun.* **1989**, *73*, 91−95.
(13) Dutta, A. K.; Kamada, K.; Ohta, K. *J. Photochem. Photobiol. A* **1996**, *93*, 57−64.
(14) Grachev, A. V., Jr.; Esayan, G. M.; Ponomarev, A. N.; Rubin, L. B.; Yuzhakov, V. I. *Opt. Spectrosc.* **1991**, *70*, 804−807.
(15) Verkhovskaja, K. A.; Fridkin, V. M.; Bune, A. V.; Tatikolov, A. S.; Legrand, J. F. *J. Appl. Phys.* **1994**, *75*, 663−665.
(16) Palazzotto, M. C.; Sahyun, M. R. V.; Serpone, N.; Sharma, D. K. *J. Chem. Phys.* **1989**, *90*, 3373−3379.
(17) Deshpande, A. V.; Namdas, E. B. *J. Lumin.* **2000**, *91*, 25−31.
(18) Reisfeld, R.; Zusman, R.; Cohen, Y.; Eyal, M. *Chem. Phys. Lett.* **1988**, *147*, 142−147.
(19) Fukuda, M.; Kodama, K.; Yamamoto, H.; Mito, K. *Dyes Pigments* **2002**, *53*, 67−72.
(20) Fayed, T. A.; Organero, J. A.; Garcia-Ochoa, I.; Tormo, L.; Douhal, A. *Chem. Phys. Lett.* **2002**, *364*, 108−114.
(21) Yariv, E.; Schultheiss, S.; Saraidarov, T.; Reisfeld, R. *Opt. Mater.* **2001**, *16*, 29−38.
(22) Costela, A.; Garcia-Moreno, I.; Barroso, J.; Sastre, R. *Appl. Phys. B* **2000**, *70*, 367−373.
(23) Costela, A.; Florido, F.; Garcia-Moreno, I.; Duchowicz, R.; Amat-Guerri, F.; Figuera, J. M.; Sastre, R. *Appl. Phys. B* **1995**, *60*, 383−389.
(24) Costela, A.; Garcia-Moreno, I.; Sastre, R.; Arbeloa, F. L.; Arbeloa, T. L.; Arbeloa, I. L. *Appl. Phys. B* **2001**, *73*, 19−24.
(25) Gupta, B. D.; Ratnanjali *Sens. Actuators, B* **2001**, *80*, 132−135.
(26) Cullum, B. M.; Mobley, J.; Bogard, J. S.; Moscovitch, M.; Philips, G. W.; Vo-Dinh, T. *Anal. Chem.* **2000**, *72*, 5612−5617.
(27) Pham, V. P.; Galstyan, T.; Granger, A.; Lessard, R. A. *Jpn. J. Appl. Phys.* **1997**, *36*, 429−438.

(28) Mansour, A. F. *Polym. Test* **2003**, *22*, 491−495.
(29) Mansour, A. F.; El-Shaarawy, M. G.; El-Bashir, S. M.; El-Mansy, M. K.; Hammam, M. *Polym. Test* **2002**, *21*, 277−281.
(30) Müller, M.; Zentel, R.; Maka, T.; Romanov, S. G.; Sotomayor Torres, C. M. *Chem. Mater.* **2000**, *12*, 2508−2512.
(31) Wadsworth, W. J.; Griffin, S. M.; McKinnie, I. T.; Sharpe, J. C.; Woolhouse, A. D.; Haskell, T. G.; Smith, G. *Appl. Opt.* **1999**, *38*, 2504−2509.
(32) Costela, A.; Garcia-Moreno, I.; Barroso, J.; Sastre, R. *Appl. Phys. B* **1998**, *67*, 167−173.
(33) El-Shahawy, M. A.; Mansour, A. F.; Hashem, H. A. *Ind. J. Pure Appl. Phys.* **1998**, *36*, 78−84.
(34) Kalogeras, I. M. *Polymer* **2003**, *44*, 4817−4827.
(35) Kalogeras, I. M.; Vassilikou-Dova, A. *J. Phys. Chem. B* **2001**, *105*, 7651−7662.
(36) El-Shahawy, M. A. *Polym. Test* **1999**, *18*, 389−396.
(37) El-Shahawy, M. A. *Polym. Test* **2000**, *19*, 821−829.
(38) Kalogeras, I. M.; Vassilikou-Dova, A. *Mater. Res. Innovations* **2003**, *7*, 263.
(39) El-Shaarawy, M. G.; Mansour, A. F.; El-Bashir, S. M.; El-Mansy, M. K.; Hammam, M. *J. Appl. Polym. Sci.* **2003**, *88*, 793−805. Mansour, A. F.; El-Shaarawy, M. G.; El-Bashir, S. M.; El-Mansy, M. K.; Hammam, M. *Polym. Int.* **2002**, *51*, 393−397.
(40) Lei, D.; Runt, J.; Safari, A.; Newnam, R. E. *Macromolecules* **1987**, *20*, 1797−1801.
(41) Brower, S. C.; Hayden, L. M. *J. Polym. Sci., Part B: Polym. Phys.* **1998**, *36*, 1013−1024.
(42) Strutz, S. J.; Brower, S. C.; Hayden, L. M. *J. Polym. Sci., Part B: Polym. Phys.* **1998**, *36*, 901−911.
(43) Ribiere, J.-C.; Lager, L.; Fort, A.; Méry, S. *Macromolecules* **2003**, *36*, 2516−2525.
(44) Because of their common origin from perylene, it is possible to describe both the perylene and the perylimide derivatives as "perylenes" (Seybold, G.; Wagenblast, G. *Dyes Pigments* **1989**, *11*, 303−317). For clarity, this generalization has been avoided here.
(45) Van Turnhout, J. *Thermally Stimulated Discharge of Polymer Electrets*; Elsevier: Amsterdam, 1975.
(46) Vanderschueren, J.; Gasiot, J. Field-Induced Thermally Stimulated Currents. In *Topics in Applied Physics*; Sessler, G. M., Ed.; Springer: Berlin, 1980.
(47) Hedvig, P. *Dielectric Spectroscopy of Polymers*; Wiley: New York, 1977.
(48) Muzeau, E.; Perez, J.; Johari, G. P. *Macromolecules* **1991**, *24*, 4713−4723.
(49) Bergman, R.; Alvarez, F.; Alegría, A.; Colmenero, J. *J. Non-Cryst. Solids* **1998**, *235−237*, 580−583.
(50) Schmidt-Rohr, K.; Kulik, A. S.; Beckham, H. W.; Ohlemacher, A.; Pawelzik, U.; Boeffel, C.; Spiess, H. W. *Macromolecules* **1994**, *27*, 4733−4745.
(51) Drotning, W. D.; Roth, E. P. *J. Mater. Sci.* **1989**, *24*, 3137−3140.
(52) Shi, W.; Fang, C.; Pan, Q.; Sun, X.; Gu, Q.; Xu, D.; Yu, J. *React. Funct. Polym.* **2000**, *44*, 177−182.
(53) Kalogeras, I. M. Ph.D. Thesis, University of Athens, 2000 (unpublished).
(54) Starkweather, H. W. *Macromolecules* **1988**, *21*, 1798−1802.
(55) Starkweather, H. W. *Macromolecules* **1990**, *23*, 328−332.
(56) Ishida, Y.; Yamafuji, K. *Kolloid-Z.* **1961**, *177*, 97.
(57) Neagu, R. M.; Neagu, E. R.; Kalogeras, I. M.; Vassilikou-Dova, A. *Mater. Res. Innovations* **2001**, *4*, 115−125.
(58) Neagu, E. R.; Neagu, R. *J. Phys. D: Appl. Phys.* **2002**, *35*, 2298−2303.
(59) Neagu, E. R.; Neagu, R. *Thermochim. Acta* **2003**, *395*, 183−189.
(60) Neagu, E. R. *Thermochim. Acta* **2003**, *402*, 37−43.
(61) Kalogeras, I. M.; Vassilikou-Dova, A.; Neagu, E. R. *Mater. Res. Innovations* **2001**, *4*, 322−333 and references therein.
(62) Kumar, G. A.; Thomas, V.; Jose, G.; Unnikrishnan, N. V.; Nampoori, V. P. N. *J. Photochem. Photobiol. A* **2002**, *153*, 145−151.
(63) Rahn, M. D.; King, T. A. *SPIE Sol-Gel Opt. III* **1994**, *2288*, 382−386.
(64) Qian, G.; Yang, Y.; Wang, Z.; Yang, C.; Yang, Z.; Wang, M. *Chem. Phys. Lett.* **2003**, *368*, 555−560.
(65) Billmeyer, F. W., Jr. *Textbook of Polymer Science*; Wiley & Sons: Singapore, 1984.
(66) Popov, S. *Appl. Opt.* **1998**, *37*, 6449−6455.
(67) Amat-Guerri, F.; Costela, A.; Figuera, J. M.; Florido, F.; Sastre, R. *Chem. Phys. Lett.* **1993**, *209*, 352−356.
(68) Gromov, T. A.; Dynmaev, K. M.; Maneknov, A. A.; Masluukov, A. P.; Matyushin, G. A.; Nechitalio, V. S.; Prokhorov, A. M. *J. Opt. Soc. Am. B* **1985**, *2*, 1028−1031.
(69) Vogel, M.; Rettig, W.; Sens, R.; Drexhage, K. H. *Chem. Phys. Lett.* **1988**, *147*, 461−465.
(70) Homilius, F.; Heilmann, A.; Rempel, U.; Von Borczyskowski, C. *Vacuum* **1998**, *49*, 205−211.

MA035299V